The FASEB Journal article fj.15-270975. Published online July 1, 2015.

The galectin-1–glycan axis controls sperm fertilizing capacity by regulating sperm motility and membrane hyperpolarization

Gustavo Vasen,* Maria Agustina Battistone,*,[1] Diego O. Croci,*,[1] Nicolás G. Brukman,* Mariana Weigel Muñoz,* Juan C. Stupirski,* Gabriel A. Rabinovich,*,† and Patricia S. Cuasnicú*,[2]

*Instituto de Biología y Medicina Experimental (IBYME-CONICET), Buenos Aires, Argentina; and †Facultad de Ciencias Exactas y Naturales, Universidad de Buenos Aires, Buenos Aires, Argentina

ABSTRACT **Lectin–glycan recognition systems play central roles in many physiologic and pathologic processes. We identified a role for galectin-1 (Gal-1), a highly conserved glycan-binding protein, in the control of sperm function. We found that Gal-1 is expressed in the epididymis and associates with sperm during epididymal maturation. Exposure of sperm to Gal-1 resulted in glycan-dependent modulation of the acrosome reaction (AR), a key event in the fertilization process. Gal-1-deficient (*Lgals1*$^{-/-}$) mice revealed the essential contribution of this lectin for full sperm fertilizing ability both *in vitro* and *in vivo*. Mechanistically, *Lgals1*$^{-/-}$ sperm exhibited defects in their ability to develop hyperactivation, a vigorous motility required for penetration of the egg vestments. Moreover, *Lgals1*$^{-/-}$ sperm showed a decreased ability to control cell volume and to undergo progesterone-induced AR, phenotypes that were rescued by exposure of the cells to recombinant Gal-1. Interestingly, the AR defect was associated with a deficiency in sperm membrane potential hyperpolarization. Our study highlights the relevance of the Gal-1–glycan axis in sperm function with critical implications in mammalian reproductive biology.—Vasen, G., Battistone, M. A., Croci, D. O., Brukman, N. G., Weigel Muńoz M., Stupirski, J. C., Rabinovich, G. A., Cuasnicú, P. S. The Gal-1–glycan axis controls sperm fertilizing capacity by regulating sperm motility and membrane hyperpolarization. *FASEB J.* 29, 000–000 (2015). www.fasebj.org**

Key Words: acrosome reaction · capacitation · fertilization · glycosylation

Programmed remodeling of cell surface glycans through the coordinated action of glycosyltransferases and glycosidases is a hallmark of a wide array of biologic processes, including embryogenesis, angiogenesis, and immunity (1). Research over the past few years has enabled the characterization of the glycome—that is, the complete repertoire of glycans—of several tissues including the human sperm (2, 3) and the zona pellucida (ZP) that surrounds the egg (4). Interestingly, genetic disruption of the gene encoding the mannosyl α-1,3-glycoprotein β-1,2-*N*-acetylglucosaminyltransferase, a glycosyltransferase responsible for generating hybrid and complex *N*-glycans, in the oocyte demonstrated a critical role for these glycan structures in the generation of developmentally competent oocytes (5). In addition, oocyte-specific ablation of both core-1 *O*-glycans and complex and hybrid *N*-glycans resulted in premature ovarian failure (6). Moreover, the process of sperm binding to the ZP has been proposed to be mainly carbohydrate dependent (7), suggesting that complex *N*-glycans or *O*-glycans may play key roles in sperm–egg interaction. However, oocytes deficient in either core 1/core 2 *O*-glycans or complex or hybrid *N*-glycans show normal sperm binding to the ZP (8, 9). Moreover, recent evidence suggests that a specific protein domain on ZP2 would be responsible for sperm recognition of the ZP in both murine and human oocyte (10).

Deciphering the biologic information encoded by the glycome is a role assigned to endogenous glycan-binding proteins or lectins, which play key roles in cell–cell recognition, communication, and signaling (11). Galectins, an evolutionarily conserved family of animal lectins, control cellular processes through recognition of N-acetyl-lactosamine-extended structures on complex branched *N*-glycans or core-2 *O*-glycans (12). These soluble lectins, released by several mammalian cells, contribute to cellular communication by forming multivalent lectin–glycan complexes that serve as scaffolds for organizing plasma membrane domains and modulating signaling threshold of relevant glycosylated receptors (13). Galectin-1 (Gal-1), a prototype

Abbreviations: AR, acrosome reaction; BSA, bovine serum albumin; COC, cumulus–oocyte complexes; $DiOC_6(3)$, (3-3′-dihexyloxacarbocyanine iodide); ECM, extracellular matrix; FD, fractal dimension; Gal-1, galectin-1; HEPES, (4-(2-hydroxyethyl)-1-piperazineethanesulfonic acid; LRRC52, leucine-rich-repeat-containing protein 52; P_4, progesterone;

(*continued on next page*)

[1] These authors contributed equally to this work.

[2] Correspondence: Instituto de Biología y Medicina Experimental (IBYME-CONICET), Vuelta de Obligado 2490, C1428ADN, Buenos Aires, Argentina. E-mail: pcuasnicu@ibyme.conicet.gov.ar

doi: 10.1096/fj.15-270975

This article includes supplemental data. Please visit *http://www.fasebj.org* to obtain this information.

member of this family, is abundantly expressed within the male and female reproductive tracts (14–17), and plays key roles in reproductive processes including implantation (18), placentation and fetal growth (19), vascularization (20), and immune tolerance (21–23). However, in spite of considerable progress, the role of Gal-1–glycan recognition systems in gamete biology and fertilization remains largely unexplored.

In this study, we investigated the presence and function of endogenous Gal-1 in male and female murine gametes and examined its potential implications in the fertilization process.

MATERIALS AND METHODS

Animals

Gal-1-deficient (*Lgals1*$^{-/-}$) mice were provided by F. Poirier (Jacques Monod Institute, Paris) and were bred at the Institute of Biology and Experimental Medicine (Buenos Aires, Argentina). C57BL/6 *WT* and *Lgals1*$^{-/-}$ adult male (aged 60–120 d) and both immature (aged 21–35 d) and young adult female (aged 30–60 d) mice were maintained at 23°C with a 12:12 light–dark cycle with *ad libitum* access to food and water. Experiments were conducted in accordance with the Guiding Principles for the Care and Use of Research Animals (National Institutes of Health) and following institutional guidelines (Institute of Biology and Experimental Medicine, CONICET).

Preparation of tissue and sperm extracts

Mouse testis, epididymis, uterus, oviduct, and ovary were homogenized in 200 to 400 μl ice-cold lysis buffer (PBS containing 5 mM EDTA, 1% w/v IGEPAL CA360, 0.5% w/v sodium deoxycholate, 0.1% w/v SDS, 1% v/v Triton X-100, 5 mM $MgCl_2$, and 10 mM (4-(2-hydroxyethyl)-1-piperazineethanesulfonic acid [HEPES], pH 7.2) plus 0.2 mM phenylmethylsulfonyl fluoride and 0.5% protease inhibitor cocktail (Sigma-Aldrich, St. Louis, MO, USA). After 30 min incubation on ice, samples were centrifuged at 15,000 *g* for 20 min at 4°C, and the supernatant was stored at −20°C until use. Protein concentration was estimated by the Bio-Rad (Hercules, CA, USA) Bradford protein assay.

For sperm protein analysis, mouse cauda epididymal sperm were allowed to disperse in PBS at 37°C or collected after *in vitro* capacitation. Caput sperm were collected using a Percoll gradient protocol (24). In brief, caput epididymal regions from several males were dissected with a needle in PBS and the suspension obtained was placed on the top of a 2-layer Percoll gradient (45–90% in PBS). After a 25 min centrifugation at 650 *g*, sperm were recovered from the halo observed between layers. Cauda sperm were subjected to the same procedure as a control. Sperm obtained by either spontaneous dispersion or by Percoll purification were washed 3 times in PBS by centrifugation at 300 *g* and before the last centrifugation were counted in a Neubauer chamber. The final pellet was resuspended in Laemmli sample buffer.

(*continued from previous page*)

PI, propidium iodide; rGal-1, recombinant galectin-1; rMFI, relative mean fluorescence intensity; RT-PCR, reverse transcriptase-PCR; RVD, regulatory volume decrease; WT, wild type; ZP, zona pellucida

In vitro sperm capacitation

For *in vitro* fertilization and acrosome reaction (AR) assays, mouse sperm was recovered by incising cauda epididymal tubules in 0.3 ml of mouse capacitation medium (25) supplemented with 0.3% bovine serum albumin (BSA) under paraffin oil. Aliquots of the original suspension were diluted in drops of fresh capacitation medium placed in tissue culture dishes, adjusting the final concentration to 5×10^6 cells/ml. Sperm suspensions were then incubated for 90 to 120 min under paraffin oil at 37°C in an atmosphere of 5% CO_2 in air. For the evaluation of protein tyrosine phosphorylation, the same procedure was followed with the exception that sperm were dispersed in modified Krebs-Ringer medium (Whitten HEPES-buffered medium containing 3 mg/ml BSA) in either capacitating (with 25 mM $NaHCO_3$) or noncapacitating conditions (without $NaHCO_3$). After the capacitation period, viability was assessed by light microscopy with Eosin Y staining (Sigma-Aldrich).

Recovery and treatment of mouse cumulus–oocyte complexes

Young adult females were superovulated by intraperitoneal injection of 5 IU of equine chorionic gonadotropin (Syntex, Buenos Aires, Argentina), followed by intraperitoneal administration of 5 IU of human chorionic gonadotropin (Sigma-Aldrich) 48 to 50 h later. Eggs were obtained from the oviducts of superovulated animals at 13 to 15 h after human chorionic gonadotropin administration. For *in vitro* fertilization assays, cumulus–oocyte complexes (COC) from contralateral oviducts were recovered in the same capacitation medium drop, were thoroughly washed, and were placed in individual 50 μl drops of fresh medium before insemination. For immunoblot or reverse transcriptase PCR (RT-PCR) analysis, COC were obtained and washed in PBS supplemented with 1% BSA. Cumulus cells, extracellular matrix (ECM) components, and oocytes were separated by incubating the COC for 3 min in 0.1% hyaluronidase (type IV; Sigma-Aldrich). Oocytes were collected by pipetting, and cumulus cells were separated from solubilized ECM by centrifugation at 300 × *g*. Cell preparations were resuspended in either Laemmli buffer for protein analysis or lysis solution for RT-PCR. ECM proteins were concentrated by precipitation with ice-cold trichloroacetic acid, washed with cold acetone, air dried, and dissolved in Laemmli buffer.

Immunoblot analysis

Protein samples were boiled for 5 min in Laemmli buffer with 70 mM 2-mercaptoethanol (Sigma-Aldrich), separated in a 10 or 15% SDS-PAGE under reducing conditions, and transferred onto nitrocellulose membranes (26) in a semidry transfer cell. After blocking with 2% skim milk in 0.1% Tween-20–PBS, membranes were probed overnight at 4°C with anti-Gal-1 polyclonal antibody (8 μg/ml), anti–β-tubulin monoclonal antibody (0.01 μg/ml, clone D66; Sigma-Aldrich), or antiphosphotyrosine monoclonal antibody (0.15 μg/ml, clone 4G10; EMD Millipore, Darmstadt, Germany) followed by the corresponding peroxidase-conjugated secondary antibody. The immunoreactive proteins were detected by the ECL Western blot kit (GE Healthcare, Waukesha, WI, USA).

ELISA for Gal-1 detection

Cauda epididymal and uterine fluid were obtained by retrograde flushing with PBS by introducing a syringe in the vas deferens or the uterotubal junction from superovulated females, respectively.

Fluids were centrifuged at 700 *g* for 10 min to remove cells and twice at 10,000 *g* for 15 min to eliminate remaining debris. Protein concentrations were determined by the Bradford method (Bio-Rad). ELISA for detection of soluble Gal-1 was performed essentially as described previously (27).

RT-PCR analysis

Total RNA from cumulus cells and oocytes was isolated with Ambion RNAqueous-Micro kit (Life Technologies, Carlsbad, CA, USA) according to the manufacturer's recommendations, reverse transcribed, and subjected to PCR using primers complementary to different exons of mouse *Lgals1* (forward: 5′-CCGAACACCGGGAACCTGCC-3′; reverse 5′-GGCGGGGCCCCTCACATAGA-3′), *Cd52* (forward: 5′-GGCCTGCAGACTGTCCTGAACTC-3′; reverse 5′-GGAAACTGCAGGCACCCGCATC-3′) and *Hprt1* (forward: 5′-AGTCCCAGCGTCGTGATTAGCG-3′; reverse 5′-GGGCCACAATGTGATGGCCTCC-3′) genes.

Preparation of recombinant Gal-1

Recombinant Gal-1 (rGal-1) was produced and purified as described elsewhere (28). For biotinylation, purified rGal-1 was incubated with freshly prepared 3-sulfo-NHS-Biotin (Sigma-Aldrich) in PBS at a biotin/protein ratio of 20:1 at room temperature for 30 min. The reaction was quenched by the addition glycine in PBS (0.05 M final concentration). Biotinylated Gal-1 was then dialyzed against PBS or capacitation media and stored at −20°C until use.

In vitro fertilization assays

Mouse COC derived from contralateral oviducts of each female were inseminated in different drops with capacitated sperm from each genotype (final concentration, 0.7×10^6 cells/ml) and gametes were coincubated at 37°C and 5% CO_2 for 24 h. After this period, the number of 2-cell embryos was observed by optical microscopy, and the percentage of fertilization was calculated (at least 3 females of each genotype per experiment).

In vivo fertilization

Immature females were superovulated as described above, and immediately after human chorionic gonadotropin injection (early in the afternoon) were individually caged with a sexually mature male. The following morning, females were checked for vaginal plugs, and eggs were recovered from the ampulla, fixed with 2% paraformaldehyde, stained with 10 μg/μl Hoechst dye 33342 (Sigma-Aldrich), and examined under a Nikon Optiphot microscope (Nikon, Tokyo, Japan) equipped with epifluorescence optics (×250). Eggs were considered fertilized if 1 decondensing sperm nucleus or 2 pronuclei were observed in the cytoplasm. In all cases, the males were subjected to 2 consecutive matings.

Gal-1 binding assay

Sperm recovered in PBS were fixed with paraformaldehyde 4% in PBS for 10 min and washed 3 times with PBS supplemented with 4 mg/ml BSA. Sperm (2×10^6) were incubated with 0 to 30 μM biotinylated Gal-1 in the absence or presence of 30 mM β-lactose (Sigma-Aldrich) or sucrose (Baker, Phillipsburg, NJ, USA) for 1 h at 37°C. Then cells were washed twice with PBS and exposed to streptavidin–FITC (1:50, Sigma-Aldrich) for 30 min at 37°C, as described elsewhere (29). Finally, sperm were washed, resuspended in PBS, and analyzed in a BD FACSAria II flow cytometer (BD Biosciences, San Jose, CA, USA). Relative mean fluorescence intensity (rMFI) was calculated by subtracting and dividing the geometric mean fluorescence intensity of each treatment by the corresponding control value (without protein). For apparent K_D determination, the rMFI obtained for each point in the presence of lactose was subtracted from the corresponding control (only Gal-1) value (to estimate nonspecific binding), normalized to the maximum signal and fitted to a hyperbolic 1–binding site model. For localization studies, the samples used for flow cytometry were mounted on slides and examined under a Nikon Optiphot microscope equipped with epifluorescence optics (×400).

AR assay

For each treatment, 50 μl of capacitation drops were prepared in the same dish covered with mineral oil. To evaluate the ability of Gal-1 to induce AR, sperm (5×10^6 cells/ml) were incubated during the capacitation period with 8 μM purified Gal-1 (previously dialyzed against medium) in the absence or presence of 30 mM β-lactose. For induction of AR, 50–100 μM progesterone (P_4) (Sigma-Aldrich), 80 mM KCl, 10 μM ionophore A23187 (Sigma-Aldrich), or 1 μM valinomycin (Sigma-Aldrich) were added, and sperm were incubated 30 min at 37°C and 5% CO_2. The AR was assessed by Coomassie Brilliant Blue staining, as described elsewhere (30). Sperm were fixed in 4% (v/v) paraformaldehyde in PBS for 15 min at room temperature, washed with 0.1 M ammonium acetate (pH 9.0), mounted on slides, and air dried. Slides were washed by successive immersions in water, methanol, and water (5 min each) and were then incubated in 0.22% Coomassie Brilliant Blue solution (50% methanol and 10% acetic acid). After staining, slides were thoroughly washed with distilled water, air dried, mounted with glycerol, and immediately observed to avoid diffusion of the stain. Sperm were scored as acrosome intact when a bright blue staining was observed on the dorsal region of the acrosome or as reacted acrosome when staining was absent. At least 600 sperm were counted for each condition.

Analysis of osmotic effects on cell morphology

Capacitated sperm morphology was assessed by placing 10 μl cells on prewarmed slides, and videos were recorded in a phase-contrast Nikon microscope (×400). At least four 35-s videos, acquired at 30 Hz frame rate, were evaluated to allow examination of 200 sperm. To evaluate the effect of medium osmolarity in sperm morphology, different media were prepared as described elsewhere (31). In brief, sperm were isolated in 200 μl 430-mOsM Hepes-buffered saline (HS), pH 7.4 medium (5 mM KCl, 1 mM $MgSO_4$, 2 mM $CaCl_2$, 20 mM HEPES, 5 mM glucose, 10 mM lactic acid, and 1 mM sodium pyruvate adjusted with NaCl to yield the desired osmolarity) and then diluted into 430 or 310 mOsM HS medium (final osmolarity). After 15 min incubation at 37°C, motility and morphology were evaluated. The hairpin percentage was calculated by classifying motile sperm into hairpin or straight morphology categories.

Analysis of sperm motility

Aliquots (10 μl) of sperm capacitated in the presence or absence of rGal-1 were placed on prewarmed slides and motility recorded at 30 Hz with a Nikon Coolpix L20 camera in a Nikon

Eclipse TS100 microscope using LWD 20×/0.40 Ph1 ADL ∞/1.2 WD 3.0 objective lenses. Sperm trajectories were then manually tracked using the MtrackJ plug-in (www.imagescience.org/meijering/software/mtrackj/) for ImageJ software (version 1.47; National Institutes of Health, Bethesda, MD, USA). The tracks were analyzed with R (version 3.0.3, http://cran.r-project.org/). For each sperm, the *x* and *y* positions corresponding to 31 points (1 s) were used for calculating the linear and curvilinear velocities and fractal dimension (FD) (32). Motility patterns were classified as linear (FD ≤ 1.3; trajectories with almost no fluctuations from the line) or hyperactivated (FD > 1.65; star-spin trajectories) (33, 34).

Assessment of membrane potential

The lipophilic voltage-sensitive dye $DiOC_6(3)$ (3,3′-dihexyloxacarbocyanine iodide; Sigma-Aldrich) was used to monitor mouse sperm membrane potential, as previously reported (35). Sperm were capacitated for 90 min at a concentration of 5×10^6 cells/ml in the presence or absence of 50 μM H89 (Sigma-Aldrich). Then sperm were centrifuged at 300 *g* for 5 min and resuspended in BSA-free capacitation media. Each sperm aliquot was first treated with 1 μM carbonyl cyanide *m*-chlorophenyl hydrazone (CCCP) for 2 min (to collapse mitochondrial membrane potential) and then with 5 nM $DiOC_6(3)$ and 0.25 μg/ml propidium iodide (PI) for exactly 2 min and finally analyzed by flow cytometry. $DiOC_6(3)$ and PI were excited with a 488 nm argon laser, and 50,000 events were collected for each condition. Data analysis was performed by R software. Given the variability of mean fluorescence between duplicates, the $DiOC_6(3)$ fluorescence intensity was normalized. The percentage of hyperpolarized sperm was calculated by analyzing the histograms of $DiOC_6(3)$ fluorescence intensity of live wild-type (WT) cells (PI negative) and choosing a threshold value that separated the capacitated and noncapacitated sperm populations (36).

Statistical analysis

Results are expressed as mean values ± SEM for each series of experiments. The Student *t* test or ANOVA with Tukey posttest were used to evaluate significance.

RESULTS

Presence of Gal-1 in male and female reproductive tissues and gametes

We first assessed the presence of Gal-1 in male gametes and reproductive organs using a specific anti-Gal-1 antibody (27). We identified Gal-1 in the testis and the epididymis of WT mice (**Fig. 1*A***). Notably, expression of epididymal Gal-1 was segment regulated, increasing from caput to cauda (Fig. 1*B*). Moreover, soluble Gal-1 was quantified by ELISA in epididymal fluid (2.6 ± 1.5 ng Gal-1/μg total protein; $n = 3$) and identified in fresh cauda but not caput epididymal sperm (Fig. 1*C*, left and middle), indicating that the secreted protein binds to sperm during epididymal maturation. Interestingly, Gal-1 remains associated with sperm subjected to capacitation (Fig. 1*C*, right), a process that takes place in the female tract and renders sperm capable of fertilizing the egg. Examination of testicular and epididymal tissues from Gal-1-deficient ($Lgals1^{-/-}$) mice revealed normal seminiferous and epididymal tubules with abundant sperm in the lumen, whereas the analysis of epididymal sperm revealed no differences in their number or viability compared to their WT counterpart (Supplemental Fig. S1). Within the female reproductive tract, we identified Gal-1 protein in mouse ovary, oviduct, and uterus (Fig. 1*D*),

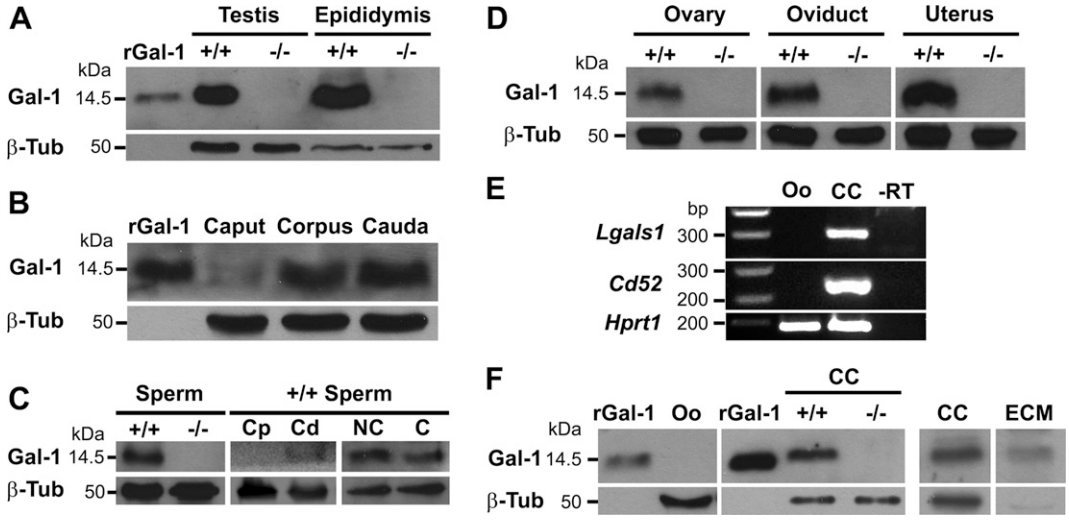

Figure 1. Presence of Gal-1 in male and female reproductive organs and gametes. *A–D, F*) Western blot analysis of Gal-1 and β-tubulin (β-tub). *A*) Testicular and epididymal lysates (75 μg/lane) from WT ($^{+/+}$) and $Lgals1^{-/-}$ ($^{-/-}$) mice. rGal-1 was used as positive control. *B*) Lysates from 3 main epididymal segments (caput, corpus, cauda). *C*) Protein lysates from cauda epididymal WT and $Lgals1^{-/-}$ sperm (4×10^6 cells/lane, left), caput (Cp), and cauda (Cd) WT sperm (2×10^6 cells/lane, middle) and noncapacitated (NC) or capacitated (C) WT sperm (4×10^6 cells/lane, right). *D*) Protein lysates from uterus, oviduct, and ovary from WT and $Lgals1^{-/-}$ mice. *E*) RT-PCR of total RNA from oocytes (Oo) and cumulus cells (CC) using *Cd52* and *Hprt1* genes as purity and loading controls, respectively. The product of RT reaction without retrotranscription (−RT) was used to exclude possible amplification of genomic sequences and/or pseudogenes. *F*) Western blot analysis of protein lysates from oocytes (Oo) and cumulus cells (CC) from 40 WT or $Lgals1^{-/-}$ COC (left) and of trichloroacetic acid-precipitated proteins from ECM of hyaluronidase-treated COC and corresponding cumulus cells (CC) (right). Anti-β-tubulin was used as control of contaminating cells in ECM fraction.

as well as in the uterine fluid by ELISA (2.7 ± 0.5 ng Gal-1/μg total protein; $n=5$). Analysis of cumulus cells and oocytes isolated from COC revealed the presence of *Lgals1* mRNA in cumulus cells but not in oocytes, even when high amounts of cDNA were used as input (Fig. 1*E*). To exclude the possibility that oocyte preparation could be contaminated with cumulus cells, the presence of *Cd52* mRNA, a transcript specifically expressed in cumulus cells (37), was used as a control. In agreement with mRNA expression, immunoblot analysis revealed the presence of Gal-1 protein in cumulus cells and cumulus ECM but not in oocyte lysates (Fig. 1*F*). Thus, Gal-1 is differentially regulated in male and female reproductive tissues and fluids, suggesting its potential role in controlling gamete biology.

Gal-1 influences the AR in a carbohydrate-dependent manner

Given the prominent expression of Gal-1 at sites of sperm capacitation and fertilization and its presence in cumulus cells, we then examined the ability of this lectin to modulate sperm function. Biotinylated recombinant Gal-1 (rGal-1) bound to fresh cauda epididymal sperm in a carbohydrate-dependent manner, as β-lactose (a specific galectin disaccharide) but not sucrose (a nonrelated disaccharide), prevented Gal-1–sperm interactions (**Fig. 2*A***). Accordingly, exposure to β-lactose resulted in reduced binding of rGal-1 to both the head (*i.e.,* dorsal and postacrosomal regions) and the tail of the cells (Fig. 2*B*). Subsequent analysis revealed that rGal-1 associates with sperm with an apparent K_D of 12 μM (Fig. 2*C*).

To examine whether exposure of sperm to rGal-1 influences the functional state of these cells, we investigated the effects of this lectin on sperm capacitation by evaluating the percentage of AR, a key exocytotic event essential for different stages of the fertilization process. Although rGal-1 did not affect sperm viability (rGal-1, 51.1 ± 1.6% *vs.* control, 51.9 ± 1.8%, $n=5$), exposure to this lectin during the capacitation process significantly increased the percentage of AR (Fig. 2*D*). This effect was prevented when sperm cells were incubated with rGal-1 in the presence of lactose, indicating that rGal-1 increases the percentage of AR in a carbohydrate-dependent fashion. The impact of Gal-1 on the AR was further characterized by incubating sperm with rGal-1 under capacitating conditions for only 30 min (a time period that is not sufficient for completion of capacitation) or by exposing already capacitated sperm to rGal-1. Under none of these conditions did rGal-1 influence the AR (Supplemental Fig. S2), suggesting that this lectin may affect late events in the capacitation process.

Gal-1 modulates fertilization

Given the presence of Gal-1 in both gametes and the ability of this lectin to regulate sperm function, we investigated the contribution of Gal-1 to sperm-egg interaction by *in vitro* fertilization assays involving capacitated sperm and

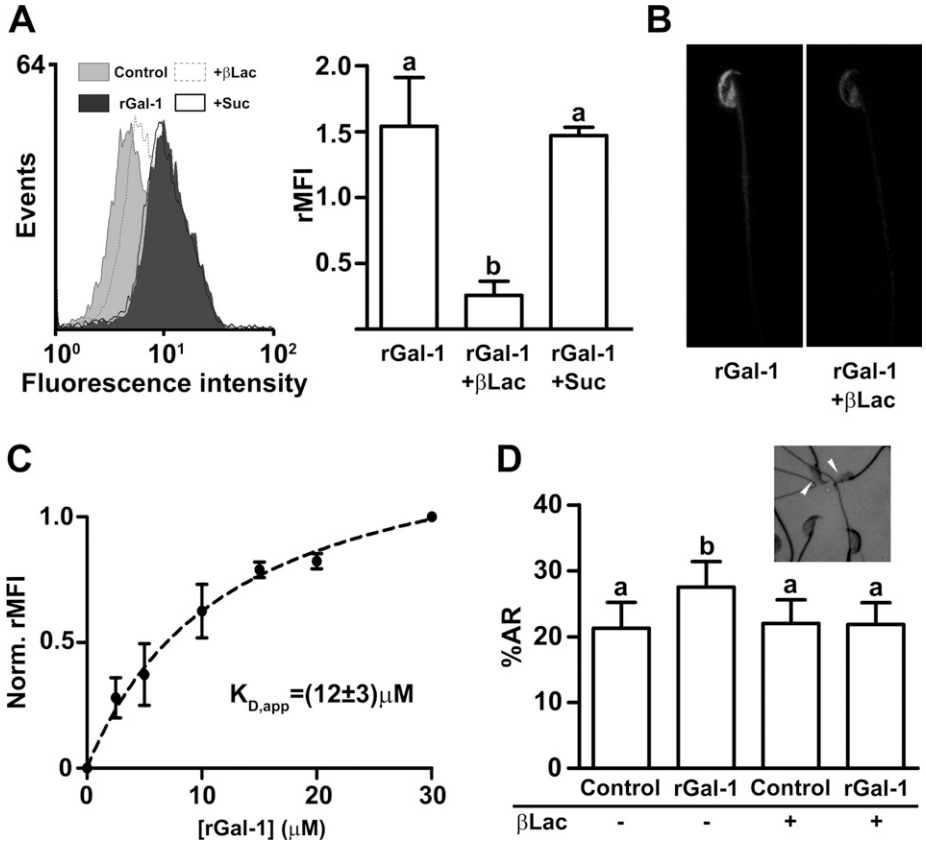

Figure 2. Effect of binding of rGal-1 on sperm function. *A*) Flow cytometry of fixed cauda epididymal sperm incubated for 60 min in medium alone (control) or medium containing 8 μM biotinylated rGal-1 in absence or presence of β-lactose (β-Lac) or sucrose (Suc; nonspecific disaccharide) and subsequently exposed to streptavidin–FITC (left). Histogram representative of 3 independent experiments (right). rMFI (right) was calculated as (mean fluorescence intensity [MFI] experimental − MFI control)/MFI control. Data are presented as means ± SEM of 3 independent experiments. (*A*) *vs.* (*B*), $P < 0.05$. *B*) Localization of rGal-1 bound to cauda sperm in absence or presence of β-lactose. *C*) Analysis of rGal-1 binding to sperm. Dashed line represents best fit to hyperbolic 1-binding site model, and resulting apparent K_D ($K_{D,app}$) is shown. Data are presented as means ± SEM of 3 independent experiments. *D*) Epididymal sperm were exposed to 8 μM rGal-1 during capacitation (90 min) in presence or absence of β-lactose. After incubation, percentage of AR was evaluated by Coomassie Brilliant Blue staining (inset; arrow indicates acrosome-reacted cells). Results represent means ± SEM of 4 independent experiments. (*A*) *vs.* (*B*), $P < 0.001$.

COC both from *Lgals1*$^{-/-}$ and WT mice. We found a substantially lower percentage of fertilization when *Lgals1*$^{-/-}$ sperm was used, regardless of the COC genotype (**Fig. 3*A***), suggesting a critical role of sperm-derived Gal-1 in sperm–egg interaction.

To investigate whether the impaired sperm fertilizing ability observed *in vitro* could also be detected under *in vivo* conditions, *Lgals1*$^{-/-}$ and WT males were mated with superovulated females, and the number of fertilized eggs recovered from the ampulla was evaluated the next day. In agreement with *in vitro* observations, fertilization rates were significantly lower for Gal-1-deficient males than control males (Fig. 3*B*, day 1). Notably, when males were subjected to a second consecutive mating, the fertilization rates of WT males remained unchanged, whereas those corresponding to *Lgals1*$^{-/-}$ males dramatically declined (Fig. 3*B*, day 2).

Mechanisms underlying Gal-1 modulation of sperm function

To explore functional differences between *Lgals1*$^{-/-}$ and WT sperm as well as potential mechanisms underlying Gal-1 regulatory effects, cells from the 2 genotypes were incubated under *in vitro* capacitating conditions, and

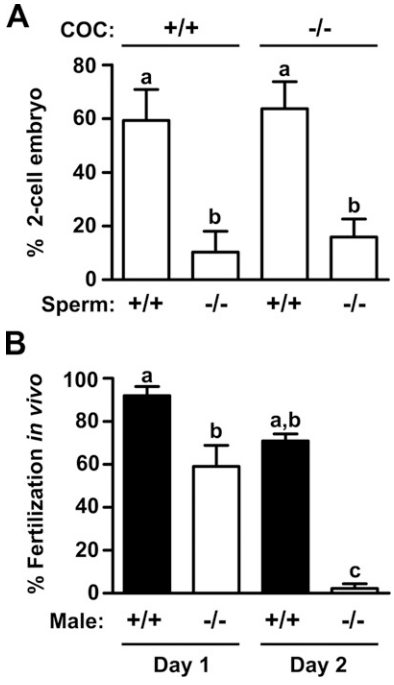

Figure 3. *In vitro* and *in vivo* fertilization performance of Gal-1-deficient gametes. *A*) WT ($^{+/+}$) and *Lgals1*$^{-/-}$ ($^{-/-}$) COC were inseminated with *in vitro* capacitated sperm from both genotypes. After 24 h coincubation, percentage of 2-cell embryos was determined. Results represent means ± SEM of 4 independent experiments. (*A*) *vs.* (*B*), $P < 0.05$. *B*) WT and *Lgals1*$^{-/-}$ males were mated with superovulated immature females. Next morning, eggs recovered from ampulla were examined for evidence of fertilization. All males were subjected to 2 consecutive matings (day 1 and day 2). Results represent means ± SEM of 3 independent experiments. (*A*) *vs.* (*B*), $P < 0.05$; (*A*) *vs.* (*C*), $P < 0.001$; (*B*) *vs.* (*C*), $P < 0.001$.

functional parameters were analyzed. No significant differences were detected in the percentage of motile sperm (**Fig. 4*A***) or their linear velocity (Fig. 4*B*). However, *Lgals1*$^{-/-}$ sperm showed reduced curvilinear velocity (Fig. 4*C*) and overall FD, an indicator of the sperm trajectory regularity (Fig. 4*D*), suggesting that mutant sperm population contains a higher number of cells with linear paths than controls. Subsequent analysis of the distribution of cells within the low and high FD intervals (Fig. 4*E*) confirmed that *Lgals1*$^{-/-}$ sperm exhibit higher levels of cells with linear trajectories than controls (Fig. 4*F*). Moreover, *Lgals1*$^{-/-}$ sperm showed decreased percentage of hyperactivation, a typical vigorous motility displayed by capacitated cells (Fig. 4*G*). In addition to differences in sperm motility patterns, a higher number of sperm with angulated tails—a phenotype known as a hairpin pattern—was observed in *Lgals1*$^{-/-}$ motile sperm populations compared to WT cells (**Fig. 5*A***). Because the hairpin pattern is associated with defects in volume regulation when sperm cells are exposed to lower osmolarity conditions (38), *Lgals1*$^{-/-}$ and WT sperm were recovered in an isosmotic medium (430 mOsM, epididymal fluid osmolarity), transferred to medium with the same or lower osmolarity (310 mOsM), and the percentage of hairpins determined 15 min after transfer. Whereas *Lgals1*$^{-/-}$ and WT sperm showed comparable percentages of hairpin cells at high osmolarity conditions, *Lgals1*$^{-/-}$ spermatozoa exhibited a percentage of angulated tails significantly higher than WT sperm when incubated in the lower osmolyte content medium (Fig. 5*B*), suggesting that Gal-1 deficiency impairs the ability of sperm to regulate their volume. Interestingly, whereas binding of rGal-1 to *Lgals1*$^{-/-}$ sperm during capacitation (Supplemental Fig. S3*A*) did not modify sperm motility behavior (Supplemental Fig. S3*B–F*), it reduced the incidence of hairpin phenotype within this population, suggesting that supplementation of this lectin partly rescues the ability of mutant sperm to regulate their volume (Fig. 5*C*).

To gain further insights into the mechanisms underlying Gal-1 function, we evaluated the effects of this lectin on other capacitation-related events. Whereas no differences were observed in protein tyrosine phosphorylation (Fig. 5*D*) or spontaneous AR (Fig. 5*E*) between *Lgals1*$^{-/-}$ and WT sperm, sperm devoid of Gal-1 failed to respond to progesterone, a well-known physiologic inducer of the AR (Fig. 5*E*). Moreover, exposure of *Lgals1*$^{-/-}$ sperm to rGal-1 did not produce an increase in AR levels as observed previously for WT sperm (Figs. 5*F* and 2*D*), although it rescued the ability of mutant sperm to respond to progesterone (Fig. 5*F*).

To further characterize the role of Gal-1 in AR induction, sperm isolated from *Lgals1*$^{-/-}$ and WT mice were exposed to the Ca^{2+} ionophore A23187 to increase the intracellular Ca^{2+} concentrations necessary for membrane fusion during the AR. Alternatively, a high extracellular K^+ concentration was applied to depolarize the plasma membrane potential, an event that enables the initiation of the AR (39). Whereas the magnitude of the AR reached in *Lgals1*$^{-/-}$ sperm treated with A23187 did not differ substantially from that observed in WT cells (**Fig. 6*A***), Gal-1-deficient sperm failed to respond to K^+ compared with control cells. Thus, Gal-1 deficiency controls intracellular Ca^{2+} elevation, a key early event associated to the AR

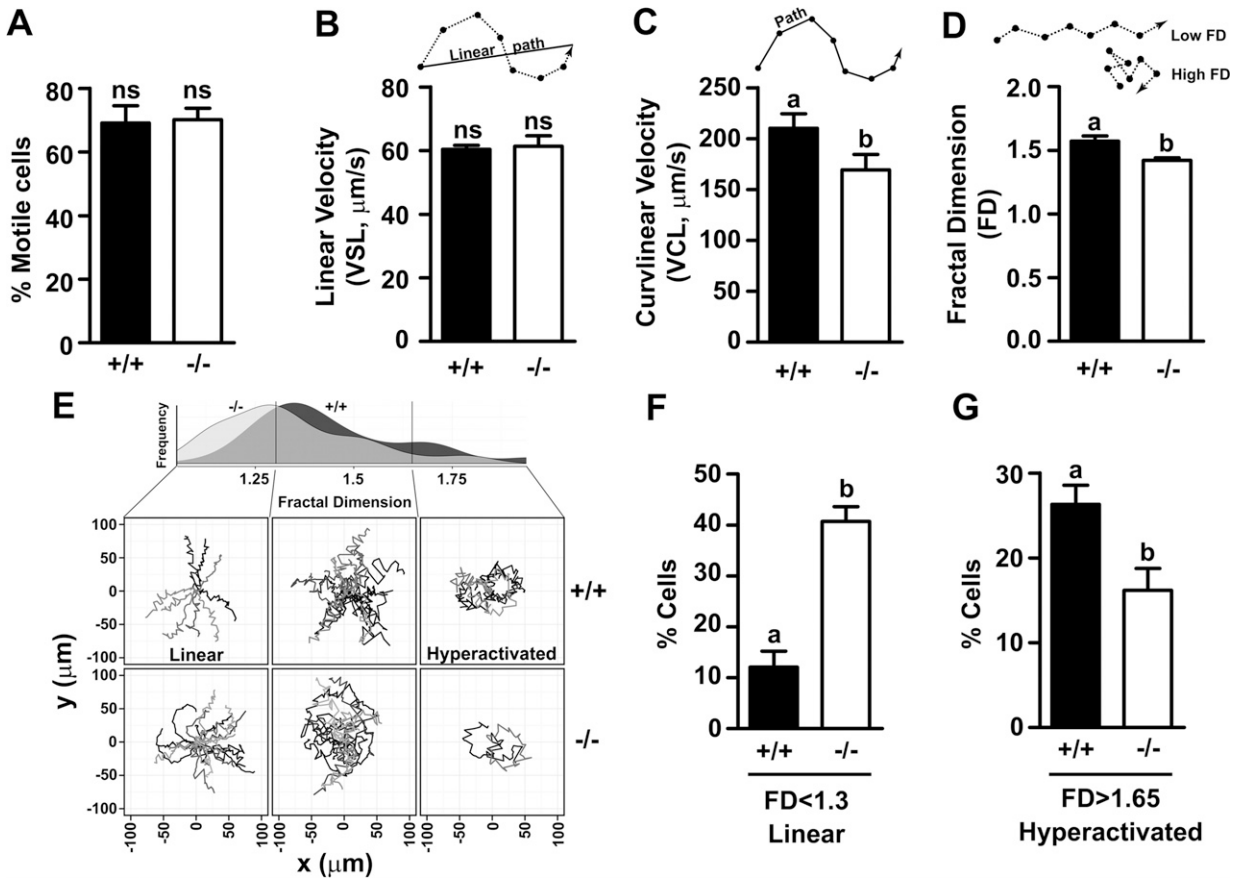

Figure 4. Impact of endogenous Gal-1 on sperm motility. *A*) Sperm from WT ($^{+/+}$) and *Lgals1*$^{-/-}$ ($^{-/-}$) mice were capacitated *in vitro* and percentage of motile cells was determined. Results represent means ± SEM of 5 independent experiments. ns, not significant. *B–D*) WT and *Lgals1*$^{-/-}$ sperm movement was tracked and linear velocity, curvilinear velocity, and FD were calculated. Results represent means ± SEM of 4 independent experiments. (*A*) *vs.* (*B*), $P < 0.05$; *E*) Representative trajectories of WT and *Lgals1*$^{-/-}$ sperm observed in different FD intervals (linear group: FD < 1.3; hyperactivated group, FD > 1.65). Representative histogram of FD distribution for both genotypes is shown in upper panel. *F, G*) Percentages of WT and *Lgals1*$^{-/-}$ cells exhibiting either linear trajectories (*A vs. B,* $P < 0.01$) or hyperactivation (*A vs. B,* $P < 0.001$). Results represent means ± SEM of 4 independent experiments.

Recent evidence indicates that hyperpolarization of the plasma membrane potential during capacitation is critical for sperm to undergo induced AR (40). To study the impact of Gal-1 in sperm plasma membrane potential, *Lgals1*$^{-/-}$ and WT sperm were treated with valinomycin, a K^+ ionophore that hyperpolarizes the sperm plasma membrane, and then exposed to progesterone. Gal-1-deficient sperm showed an increase in the percentage of AR compared to WT sperm (Fig. 6*B*). Interestingly, when the effects of valinomycin were analyzed for each of the 2 morphologic *Lgals1*$^{-/-}$ sperm populations (*i.e.,* straight and hairpin), both groups showed a deficient response to progesterone that was circumvented by valinomycin treatment, although the hairpin group exhibited a stronger phenotype being more refractory to undergo the AR (Fig. 6*C*).

On the basis of these observations, we next evaluated the percentage of hyperpolarized cells in capacitated *Lgals1*$^{-/-}$ and control sperm. Flow cytometry analysis of WT sperm using the voltage sensitive fluorescent probe $DiOC_6(3)$ revealed that only a subpopulation (~40%) of live capacitated sperm showed a decrease in membrane potential (**Fig. 7*A, C***). This decrease could be prevented by exposure of cells to H89, a PKA inhibitor that blocks the cAMP-dependent signaling cascade leading to capacitation (Fig. 7*A, C*). In contrast to their WT counterpart, capacitated *Lgals1*$^{-/-}$ cells did not show hyperpolarization (Fig. 7*B, C*), supporting the idea that Gal-1 controls the AR, at least in part, through a mechanism involving hyperpolarization of sperm plasma membrane potential.

DISCUSSION

Research over the past few years indicates that complex *N*-glycans and *O*-glycans may play key roles in sperm–egg interactions. However, the identity and molecular activities of glycan-binding partners that mediate cellular communication at the sperm–egg interface remain elusive. Because Gal-1 binds to polylactosamine-terminated glycans highly represented in the murine ZP (4), displays immune inhibitory activity at the fetomaternal interface (21, 41), and modulates signaling pathways that are critical for sperm and oocyte biology (*i.e.,* Scr kinases, integrin/FAK, and PLC-dependent Ca^{2+} mobilization) (42, 43), we hypothesized that Gal-1–glycan interactions could influence

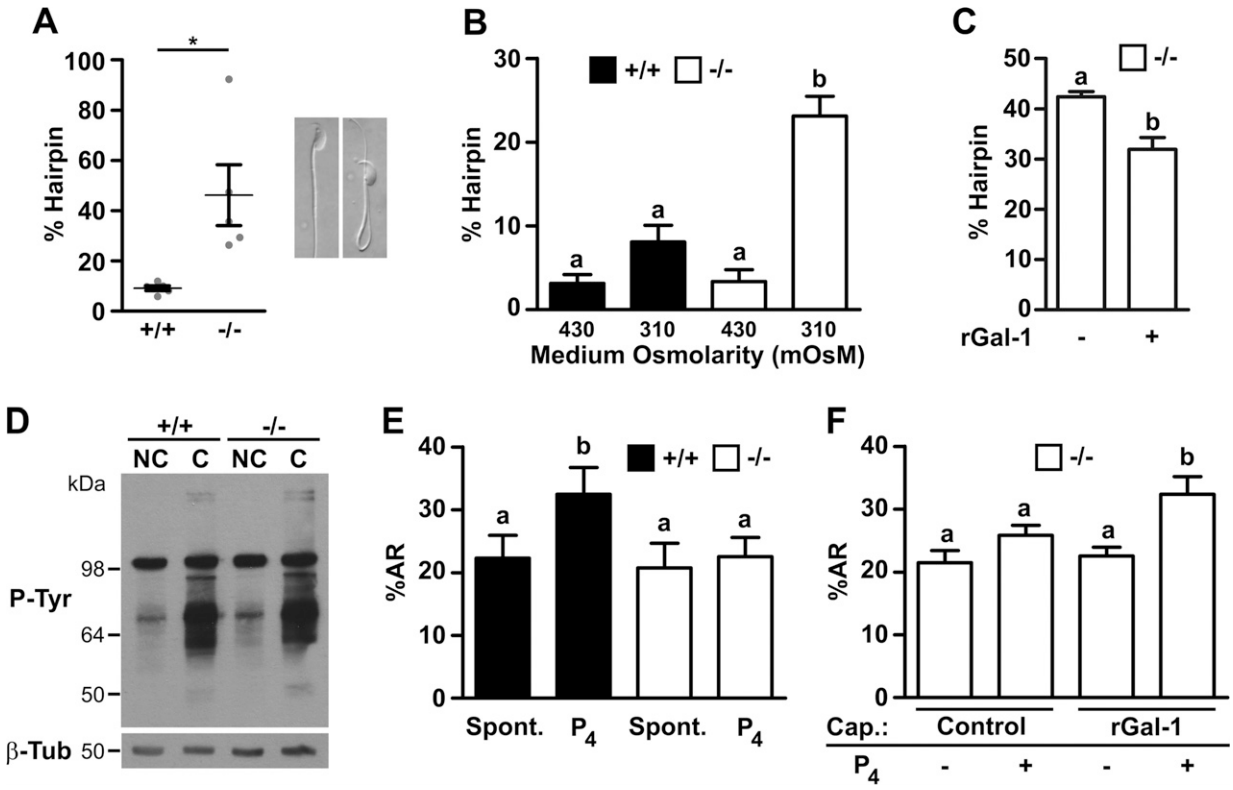

Figure 5. Relevance of endogenous Gal-1 in sperm function. *A*) Sperm from WT ($^{+/+}$) and *Lgals1*$^{-/-}$ ($^{-/-}$) mice were capacitated *in vitro* and percentage of hairpin cells was scored only within motile population. Inset corresponds to differential interference contrast images. Results represent means ± SEM of 5 independent experiments. *$P < 0.05$; *B*) Sperm from both genotypes were obtained in 430 mOsm media (isosmotic with epididymal fluid), then transferred to either 430 or 310 mOsm (isosmotic with uterine fluid and with capacitation media) solutions for 15 min, and percentage of hairpin cells was scored under microscope. Results represent means ± SEM of 3 independent experiments. (*A*) *vs.* (*B*), $P < 0.01$. *C*) *Lgals1*$^{-/-}$ sperm were exposed to 8 μM rGal-1 during capacitation, and percentage of hairpin cells was calculated. Results represent means ± SEM of 3 independent experiments. (*A*) *vs.* (*B*), $P < 0.05$. *D*) WT and *Lgals1*$^{-/-}$ sperm were incubated under noncapacitating (NC) or capacitating (C) conditions for 90 min and then subjected to immunoblot using antiphosphotyrosine (p-Tyr) or anti-β-tubulin (β-tub) antibodies. *E*) Sperm from both genotypes were *in vitro* capacitated for 90 min, followed by treatment with 50 μM P_4 for additional 30 min. Then percentage of spontaneous (Spont.) or induced percentage AR was evaluated by Coomassie Brilliant Blue staining. Results represent ± SEM of 4 independent experiments. (*A*) *vs.* (*B*), $P < 0.05$. *F*) *Lgals1*$^{-/-}$ sperm were incubated for 90 min under capacitating conditions in absence (control) or presence of 8 μM rGal-1, then exposed to 50 μM P_4 for 30 min. After incubation, percentage AR was evaluated. Results represent means ± SEM of 3 independent experiments. (*A*) *vs.* (*B*), $P < 0.05$.

gamete biology. In this study, we identified a pivotal role for Gal-1 in sperm fertilizing ability by controlling sperm motility, cell volume, and the AR through glycan-dependent mechanisms involving sperm membrane potential hyperpolarization.

Within the reproductive tracts, we found that Gal-1 was present in both the testes and the epididymis as well as in the ovary, uterus, and oviduct. Interestingly, the presence of Gal-1 in epididymal tissue was found to be segment regulated, increasing from caput to cauda, suggesting a possible role for this lectin in epididymal maturation. Consistent with these findings, Gal-1 was detected in cauda epididymal sperm as reported for rat sperm (15) but not in immature caput cells, thus substantiating the involvement of this lectin in the acquisition of sperm fertilizing ability that occurs during epididymal transit. Moreover, Gal-1 was detected in capacitated sperm as well as in cumulus cells and cumulus ECM, suggesting that this lectin might be involved in gamete interactions and the paracrine regulation of COC homeostasis, as previously suggested (44). These observations, together with the presence of Gal-1 in male and female reproductive fluids, favor the idea that Gal-1 interacts with sperm during the maturation and capacitation processes. Accordingly, we found that Gal-1 associated with sperm in a carbohydrate-dependent fashion and promoted an increase in the magnitude of the AR when present during capacitation. In this regard, it is likely that the increase in the spontaneous AR occurs as a consequence of Gal-1 binding to glycosylated receptors. Accordingly, a previous study has demonstrated that cross-linking of the glycolipid G_{M1} (a putative Gal-1 receptor) modulate the AR by regulating $Ca_V2.3$ calcium channels located in the dorsal region of the sperm head (45), a membrane domain to which rGal-1 binds. Interestingly, a similar mechanism, involving G_{M1} and TRPC5 channels has been previously described for Gal-1 in T cells (46).

In vitro fertilization studies using sperm and COC from both genotypes revealed a markedly reduced fertilizing capacity of *Lgals1*$^{-/-}$ sperm compared to its WT counterpart when coincubated with either *Lgals1*$^{-/-}$ or WT COC. Although the potential contribution of cumulus-derived Gal-1 to the fertilization process cannot be excluded, these

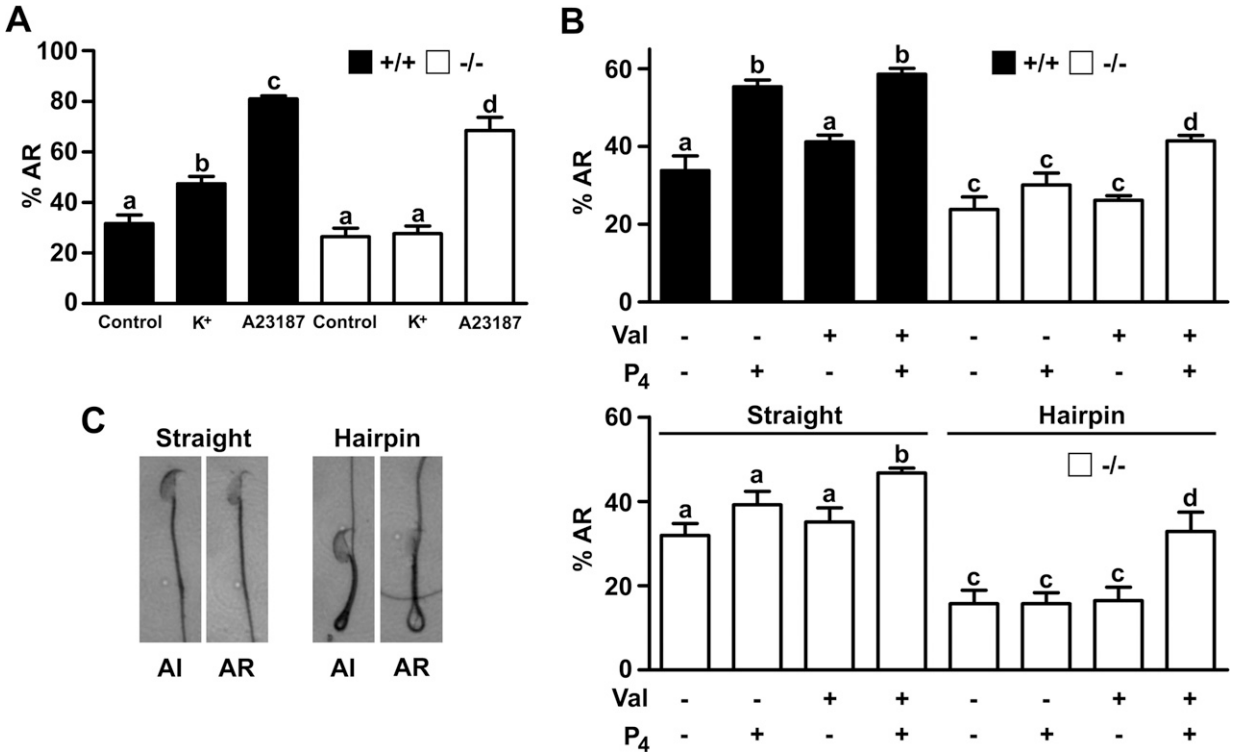

Figure 6. Molecular mechanisms underlying Gal-1 modulation of AR. *A*) WT ($^{+/+}$) and *Lgals1*$^{-/-}$ ($^{-/-}$) sperm were incubated under *in vitro* capacitating conditions for 90 min and then exposed to either 80 mM K^+ (K^+) or 10 μM calcium ionophore (A23187). Percentage of AR was then scored by Coomassie Brilliant Blue staining. Results represent means ± SEM of 4 independent experiments. (*A*) *vs.* (*B*), $P < 0.05$; (*A*) *vs.* (*C*), $P < 0.001$; (*A*) *vs.* (*D*), $P < 0.001$. *B*) Sperm from both genotypes were incubated under capacitating conditions for 90 min, then treated for 1 min with 1 μM valinomycin (Val) (at this concentration, valinomycin does not affect percentage of hairpin cells), and finally exposed to 50 μM P_4 for 30 min. After these treatments, percentage of AR was determined. Results represent means ± SEM of 3 independent experiments. (*A*) *vs.* (*B*), $P < 0.05$; (*C*) *vs.* (*D*), $P < 0.05$. *C*) *Lgals1*$^{-/-}$ sperm were treated as in (*B*) and classified as straight or hairpin while evaluating percentage of AR in each population (left). Right panel includes %AR of 4 independent experiments. (*A*) *vs.* (*B*), $P < 0.05$; (*A*) *vs.* (*C*), $P < 0.001$; (*C*) *vs.* (*D*), $P < 0.001$.

observations emphasize the relevance of sperm Gal-1 for fertilization. Notably, these *in vitro* defects could not be overcome by exposure of sperm to rGal-1 (Supplemental Fig. S4), suggesting that binding of exogenous Gal-1 to sperm is not sufficient to rescue the fertilizing ability of cells that have never been exposed to endogenous Gal-1 during epididymal maturation. In spite of the strong *in vitro* phenotype of *Lgals1*$^{-/-}$ sperm, mutant mice are fertile when naturally mated (21, 47). These results are consistent with the normal fertility levels observed in most knockout mice for sperm proteins with demonstrated roles in *in vitro* fertilization (48). In this regard, the female tract has an extremely efficient mechanism of sperm selection, leading to few but high-quality fertilizing sperm reaching the ampulla. This efficient selection system may thus mask sperm deficiencies that become evident under more restrictive conditions. Supporting this notion, we found that *Lgals1*$^{-/-}$ males exhibited *in vivo* fertilization rates significantly lower than controls when mated under more challenging conditions, such as those induced by superovulation (*i.e.,* increased number of ovulated eggs or modified sperm migration) and consecutive matings (lower number of ejaculated sperm). Thus, *in vitro* and *in vivo* experiments reveal that Gal-1-deficient sperm exhibit a clear disadvantage in their fertilizing ability compared to controls.

To investigate the mechanisms underlying the impaired sperm fertilizing ability of *Lgals1*$^{-/-}$ sperm, different functional parameters were evaluated. Analysis of sperm motility revealed that Gal-1-deficient sperm exhibit more linear trajectories and lower number of hyperactivated cells than controls. Considering that hyperactivation is required for penetration of the eggs vestments (*i.e.,* cumulus and ZP), it is likely that these motility defects contribute to the lower levels of fertilization observed *in vitro* and *in vivo.* In addition, *Lgals1*$^{-/-}$ sperm exhibited a higher percentage of angulated tails, a pattern adopted by the cells in response to an increase in the cytoplasmic volume known as the hairpin (38). When spermatozoa stored in a high osmolarity medium such as the epididymal fluid are challenged with a hypo-osmotic medium as the uterine fluid or *in vitro* capacitation media, water enters the cell and activates a mechanism termed regulatory volume decrease (RVD) (49), which involves the opening of ion channels and the release of K^+ or Cl^- to counteract the inward osmotic water flow. In sperm, it has been reported that aquaporins as well as K^+ or Cl^- channels are involved in this homeostatic response (31, 49–51). Similar to the effects observed for Gal-1, sperm RVD ability augments along the successive sections of the epididymis (52), suggesting that Gal-1 association with sperm during epididymal

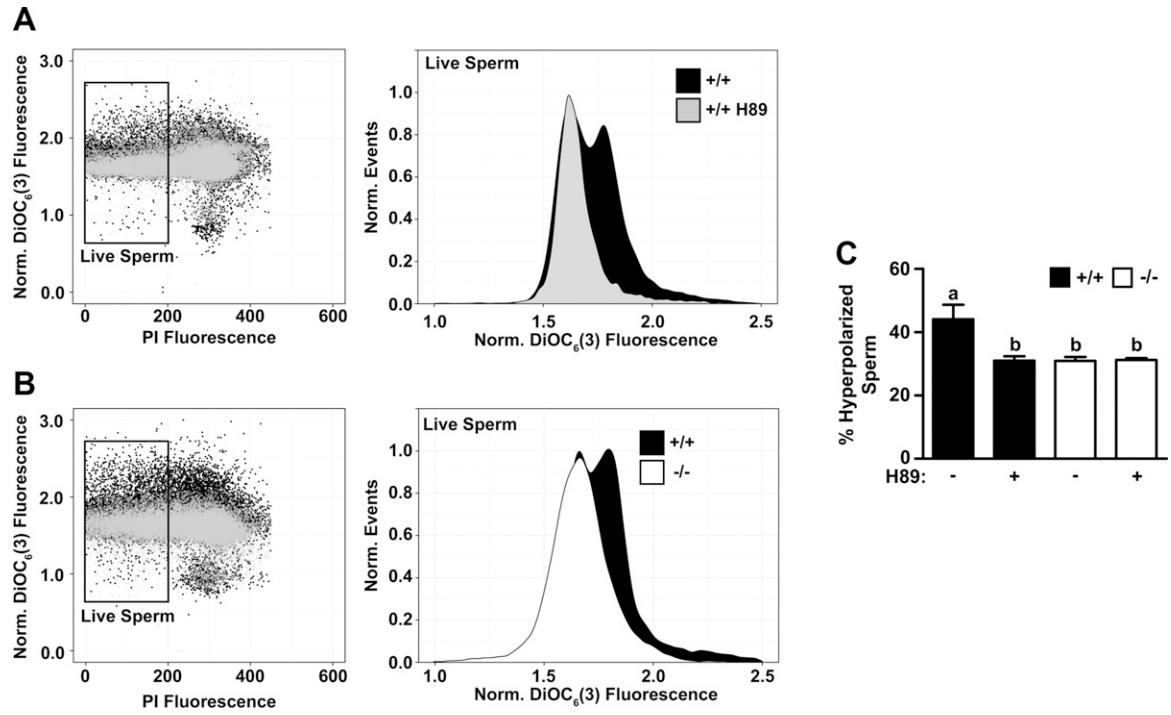

Figure 7. Involvement of endogenous Gal-1 in hyperpolarization of sperm membrane potential. *A*) WT ($^{+/+}$) sperm were capacitated in presence or absence of 50 μM H89 for 90 min, loaded with $DiOC_6(3)$ and PI, and analyzed by flow cytometry. *B*) WT and *Lgals1*$^{-/-}$ ($^{-/-}$) sperm were capacitated, and membrane potential was assessed by flow cytometry. In both (*A*) and (*B*), at left are shown representative 2-dimensional dot plots of $DiOC_6(3)$ and PI fluorescence, and at right are shown corresponding histograms of $DiOC_6(3)$ normalized (Norm) fluorescence intensity in live cells. Rectangles in dot plots indicate live (low PI) sperm populations. *C*) Percentage of hyperpolarized cells from both genotypes capacitated with or without 50 μM H89. Results represent means ± SEM of 3 independent experiments. (*A*) *vs.* (*B*), $P < 0.05$.

maturation might contribute to regulate the volume of these cells. This effect was further supported by the finding that exposure of mutant sperm to Gal-1 decreased the percentage of cells exhibiting the hairpin phenotype. Although it is tempting to speculate that the low *in vitro* fertilization rates observed for *Lgals1*$^{-/-}$ sperm are also due to defective COC penetration by hairpin-shaped sperm, previous reports in aquaporin-3-deficient mice, showed no correlation between the percentage of hairpin cells and the *in vitro* fertilization rates in each population (50).

Gal-1-deficient spermatozoa were more refractory than control cells to undergo AR, as shown by pronounced defects in their response to progesterone or higher extracellular K^+. Nonetheless, *Lgals1*$^{-/-}$ sperm reached the same AR levels than WT cells when exposed to the Ca^{2+} ionophore, indicating that AR-associated defects are placed upstream of the intracellular Ca^{2+} mobilization process required for acrosomal exocytosis. Interestingly, addition of exogenous Gal-1 to *Lgals1*$^{-/-}$ sperm during capacitation rescued progesterone-induced AR. This effect did not appear to be due to a synergistic action of Gal-1 and progesterone, as judged by the fact that Gal-1 could not increase the already high AR levels reached by progesterone induction (Supplemental Fig. S2*C, D*). Surprisingly, Gal-1 did not induce an increase in AR in *Lgals1*$^{-/-}$ sperm as previously observed for control sperm, thus emphasizing the cooperative effects of exogenous and endogenous Gal-1 in regulating the AR. These observations support the idea that specific defects in the ability of *Lgals1*$^{-/-}$ sperm to undergo the AR also contribute to the impaired fertilizing ability of these cells. In this regard, although it is well accepted that the AR is an absolute requirement for the penetration of the ZP, evidence indicates that this exocytotic event may occur either during cumulus penetration, induced by progesterone within the cumulus ECM and/or on the ZP induced by a coat glycoprotein (53). In this context, it is possible that *Lgals1*$^{-/-}$ sperm exhibit deficiencies to respond to these physiologic AR inductors at any of these fertilization stages.

Recent observations revealed that hyperpolarization of the sperm membrane potential occurring through the capacitation process is the main prerequisite for induction of the AR (40). Thus, we evaluated whether changes in plasma membrane potential hyperpolarization may account for the lower AR induction observed in Gal-1 mutant sperm treated with either progesterone or K^+. Notably, exposure of *Lgals1*$^{-/-}$ sperm to valinomycin, a K^+ ionophore that shifts membrane potential to negative values, partially bypassed the defects of these cells to undergo progesterone-induced AR. This, together with the failure of *Lgals1*$^{-/-}$ sperm to hyperpolarize during capacitation, supports the idea that Gal-1 controls the AR, at least in part, through a mechanism involving hyperpolarization of the sperm plasma membrane potential. Notably, AR defects could be overcome by valinomycin in both straight and hairpin Gal-1-deficient spermatozoa. However, the hairpin-shaped group showed a stronger phenotype with lower rates of spontaneous and progesterone-induced AR, suggesting an association between RVD and AR induction defects.

At the cellular level, Gal-1 profoundly affects trafficking, internalization, and signaling thresholds of glycosylated receptors, including VEGF receptor 2 (27), or cell surface channels, including the renal epithelial Ca^{2+} channel transient receptor potential cation channel subfamily V member 5 (54), the neuronal glutamate-gated ion channels α-amino-3-hydroxy-5-methyl-4-isoxazolepropionic acid and kainate (55), and the lymphocyte Ca^{2+} channel TRPC5 (46), suggesting that Gal-1 could function by modulating mobility or signaling channels in sperm cells too. Interestingly, Slo3, the main K^+ sperm channel, plays important roles in motility, RVD, and membrane potential control. In fact, as observed for Gal-1 mutant sperm, Slo3-deficient sperm, which do not hyperpolarize, are unable to undergo the AR, and they exhibit both motility defects and higher percentages of hairpin-shaped cells upon hypo-osmotic shock (31, 56). These observations suggest that Gal-1 might act as regulator of Slo3. This is further supported by our observations showing that Gal-1 binds to the sperm tail where Slo3 channels are expressed. Although little is known about the complex modulation of this K^+ channel activity, recent reports identified an extensively glycosylated auxiliary subunit, *i.e.,* leucine-rich-repeat-containing protein 52 (LRRC52), which modifies the channel gating behavior and is critical for fertility (57, 58) and therefore is a potential target for Gal-1. Moreover, it is possible to speculate that a Gal-1-dependent signaling complex including LRRC52 and Slo3 may function in the mechanoactivation of the channel induced by membrane stretching in RVD.

In summary, the present study demonstrates that Gal-1-deficient mice have impaired sperm fertilizing ability, defects in RVD and hyperactivation development, and a failure in their ability to undergo the AR, probably as a result of defective plasma membrane potential hyperpolarization. These findings highlight the contribution of Gal-1–glycan interactions to key events required for full sperm fertilizing ability. From a broad perspective, sperm may be considered as a good model for identifying new glycosylation-dependent processes because these transcriptionally inactive cells take advantage of posttranslational mechanisms to regulate their function. FJ

The authors thank D. J. Cohen for critical reading. This study was supported by grants from WHO-RMG (H9/TSA/037 to P.S.C.), the Argentinean National Research Council (CONICET) (PIP 2009-290 to P.S.C.), the National Agency for Promotion of Scientific and Technological Investigations (PICT 2011-2023 to P.S.C., PICT 2012-2440 to G.A.R.), and Fundación Sales (to G.A.R). G.A.R. and P.S.C. share senior authorship.

REFERENCES

1. Paulson, J. C., Blixt, O., and Collins, B. E. (2006) Sweet spots in functional glycomics. *Nat. Chem. Biol.* **2**, 238–248
2. Pang, P.-C., Tissot, B., Drobnis, E. Z., Sutovsky, P., Morris, H. R., Clark, G. F., and Dell, A. (2007) Expression of bisecting type and Lewisx/Lewisy terminated *N*-glycans on human sperm. *J. Biol. Chem.* **282**, 36593–36602
3. Xin, A.-J., Cheng, L., Diao, H., Wang, P., Gu, Y.-H., Wu, B., Wu, Y.-C., Chen, G.-W., Zhou, S.-M., Guo, S.-J., Shi, H.-J., and Tao, S.-C. (2014) Comprehensive profiling of accessible surface glycans of mammalian sperm using a lectin microarray. *Clin. Proteomics* **11**, 10
4. Easton, R. L., Patankar, M. S., Lattanzio, F. A., Leaven, T. H., Morris, H. R., Clark, G. F., and Dell, A. (2000) Structural analysis of murine zona pellucida glycans. Evidence for the expression of core 2–type *O*-glycans and the Sd(a) antigen. *J. Biol. Chem.* **275**, 7731–7742
5. Shi, S., Williams, S. A., Seppo, A., Kurniawan, H., Chen, W., Ye, Z., Marth, J. D., and Stanley, P. (2004) Inactivation of the *Mgat1* gene in oocytes impairs oogenesis, but embryos lacking complex and hybrid *N*-glycans develop and implant. *Mol. Cell. Biol.* **24**, 9920–9929
6. Williams, S. A., and Stanley, P. (2011) Premature ovarian failure in mice with oocytes lacking core 1-derived *O*-glycans and complex *N*-glycans. *Endocrinology* **152**, 1057–1066
7. Clark, G. F., and Dell, A. (2006) Molecular models for murine sperm–egg binding. *J. Biol. Chem.* **281**, 13853–13856
8. Hoodbhoy, T., Joshi, S., Boja, E. S., Williams, S. A., Stanley, P., and Dean, J. (2005) Human sperm do not bind to rat zonae pellucidae despite the presence of four homologous glycoproteins. *J. Biol. Chem.* **280**, 12721–12731
9. Williams, S. A., Xia, L., Cummings, R. D., McEver, R. P., and Stanley, P. (2007) Fertilization in mouse does not require terminal galactose or *N*-acetylglucosamine on the zona pellucida glycans. *J. Cell Sci.* **120**, 1341–1349
10. Avella, M. A., Baibakov, B., and Dean, J. (2014) A single domain of the ZP2 zona pellucida protein mediates gamete recognition in mice and humans. *J. Cell Biol.* **205**, 801–809
11. Johnson, J. L., Jones, M. B., Ryan, S. O., and Cobb, B. A. (2013) The regulatory power of glycans and their binding partners in immunity. *Trends Immunol.* **34**, 290–298
12. Rabinovich, G. A., Toscano, M. A., Jackson, S. S., and Vasta, G. R. (2007) Functions of cell surface galectin–glycoprotein lattices. *Curr. Opin. Struct. Biol.* **17**, 513–520
13. Boscher, C., Dennis, J. W., and Nabi, I. R. (2011) Glycosylation, galectins and cellular signaling. *Curr. Opin. Cell Biol.* **23**, 383–392
14. Phillips, B., Knisley, K., Weitlauf, K. D., Dorsett, J., Lee, V., and Weitlauf, H. (1996) Differential expression of two beta-galactoside-binding lectins in the reproductive tracts of pregnant mice. *Biol. Reprod.* **55**, 548–558
15. Dettin, L., Rubinstein, N., Aoki, A., Rabinovich, G. A., and Maldonado, C. A. (2003) Regulated expression and ultrastructural localization of galectin-1, a proapoptotic beta-galactoside-binding lectin, during spermatogenesis in rat testis. *Biol. Reprod.* **68**, 51–59
16. von Wolff, M., Wang, X., Gabius, H.-J., and Strowitzki, T. (2005) Galectin fingerprinting in human endometrium and decidua during the menstrual cycle and in early gestation. *Mol. Hum. Reprod.* **11**, 189–194
17. Than, N. G., Romero, R., Kim, C. J., McGowen, M. R., Papp, Z., and Wildman, D. E. (2012) Galectins: guardians of eutherian pregnancy at the maternal–fetal interface. *Trends Endocrinol. Metab.* **23**, 23–31
18. Kolundžić, N., Bojić-Trbojević, Ž., Kovačević, T., Stefanoska, I., Kadoya, T., and Vićovac, L. (2011) Galectin-1 is part of human trophoblast invasion machinery—a functional study *in vitro*. *PLoS ONE* **6**, e28514
19. Woidacki, K., Popovic, M., Metz, M., Schumacher, A., Linzke, N., Teles, A., Poirier, F., Fest, S., Jensen, F., Rabinovich, G. A., Maurer, M., and Zenclussen, A. C. (2013) Mast cells rescue implantation defects caused by *c-kit* deficiency. *Cell Death Dis.* **4**, e462
20. Freitag, N., Tirado-González, I., Barrientos, G., Herse, F., Thijssen, V. L. J. L., Weedon-Fekjær, S. M., Schulz, H., Wallukat, G., Klapp, B. F., Nevers, T., Sharma, S., Staff, A. C., Dechend, R., and Blois, S. M. (2013) Interfering with Gal-1-mediated angiogenesis contributes to the pathogenesis of preeclampsia. *Proc. Natl. Acad. Sci. USA* **110**, 11451–11456
21. Blois, S. M., Ilarregui, J. M., Tometten, M., Garcia, M., Orsal, A. S., Cordo-Russo, R., Toscano, M. A., Bianco, G. A., Kobelt, P., Handjiski, B., Tirado, I., Markert, U. R., Klapp, B. F., Poirier, F., Szekeres-Bartho, J., Rabinovich, G. A., and Arck, P. C. (2007) A pivotal role for galectin-1 in fetomaternal tolerance. *Nat. Med.* **13**, 1450–1457
22. Tirado-González, I., Freitag, N., Barrientos, G., Shaikly, V., Nagaeva, O., Strand, M., Kjellberg, L., Klapp, B. F., Mincheva-Nilsson, L., Cohen, M., and Blois, S. M. (2013) Galectin-1 influences trophoblast immune evasion and emerges as a predictive factor for the outcome of pregnancy. *Mol. Hum. Reprod.* **19**, 43–53
23. Ramhorst, R. E., Giribaldi, L., Fraccaroli, L., Toscano, M. A., Stupirski, J. C., Romero, M. D., Durand, E. S., Rubinstein, N., Blaschitz, A., Sedlmayr, P., Genti-Raimondi, S., Fainboim, L., and Rabinovich, G. A. (2012) Galectin-1 confers immune

privilege to human trophoblast: implications in recurrent fetal loss. *Glycobiology* **22**, 1374–1386
24. Krapf, D., Ruan, Y. C., Wertheimer, E. V., Battistone, M. A., Pawlak, J. B., Sanjay, A., Pilder, S. H., Cuasnicu, P., Breton, S., and Visconti, P. E. (2012) cSrc is necessary for epididymal development and is incorporated into sperm during epididymal transit. *Dev. Biol.* **369**, 43–53
25. Fraser, L. R., and Drury, L. M. (1975) The relationship between sperm concentration and fertilization *in vitro* of mouse eggs. *Biol. Reprod.* **13**, 513–518
26. Towbin, H., Staehelin, T., and Gordon, J. (1992) Electrophoretic transfer of proteins from polyacrylamide gels to nitrocellulose sheets: procedure and some applications. 1979. *Biotechnology* **24**, 145–149
27. Croci, D. O., Cerliani, J. P., Dalotto-Moreno, T., Méndez-Huergo, S. P., Mascanfroni, I. D., Dergan-Dylon, S., Toscano, M. A., Caramelo, J. J., García-Vallejo, J. J., Ouyang, J., Mesri, E. A., Junttila, M. R., Bais, C., Shipp, M. A., Salatino, M., and Rabinovich, G. A. (2014) Glycosylation-dependent lectin–receptor interactions preserve angiogenesis in anti-VEGF refractory tumors. *Cell* **156**, 744–758
28. Barrionuevo, P., Beigier-Bompadre, M., Ilarregui, J. M., Toscano, M. A., Bianco, G. A., Isturiz, M. A., and Rabinovich, G. A. (2007) A novel function for galectin-1 at the crossroad of innate and adaptive immunity: galectin-1 regulates monocyte/macrophage physiology through a nonapoptotic ERK-dependent pathway. *J. Immunol.* **178**, 436–445
29. Ilarregui, J. M., Croci, D. O., Bianco, G. A., Toscano, M. A., Salatino, M., Vermeulen, M. E., Geffner, J. R., and Rabinovich, G. A. (2009) Tolerogenic signals delivered by dendritic cells to T cells through a galectin-1-driven immunoregulatory circuit involving interleukin 27 and interleukin 10. *Nat. Immunol.* **10**, 981–991
30. Busso, D., Goldweic, N. M., Hayashi, M., Kasahara, M., and Cuasnicú, P. S. (2007) Evidence for the involvement of testicular protein CRISP2 in mouse sperm–egg fusion. *Biol. Reprod.* **76**, 701–708
31. Zeng, X.-H., Yang, C., Kim, S. T., Lingle, C. J., and Xia, X.-M. (2011) Deletion of the *Slo3* gene abolishes alkalization-activated K^+ current in mouse spermatozoa. *Proc. Natl. Acad. Sci. USA* **108**, 5879–5884
32. Mortimer, S. T., Swan, M. A., and Mortimer, D. (1996) Fractal analysis of capacitating human spermatozoa. *Hum. Reprod.* **11**, 1049–1054
33. Armon, L., and Eisenbach, M. (2011) Behavioral mechanism during human sperm chemotaxis: involvement of hyperactivation. *PLoS ONE* **6**, e28359
34. Boryshpolets, S., Pérez-Cerezales, S., and Eisenbach, M. (2015) Behavioral mechanism of human sperm in thermotaxis: a role for hyperactivation. *Hum. Reprod.* **30**, 884–892
35. Brewis, I. A., Morton, I. E., Mohammad, S. N., Browes, C. E., and Moore, H. D. (2000) Measurement of intracellular calcium concentration and plasma membrane potential in human spermatozoa using flow cytometry. *J. Androl.* **21**, 238–249
36. Escoffier, J., Navarrete, F., Haddad, D., Santi, C. M., Darszon, A., and Visconti, P. E. (2015) Flow cytometry analysis reveals that only a subpopulation of mouse sperm undergoes hyperpolarization during capacitation. *Biol. Reprod.* **92**, 121
37. Hasegawa, A., Takenobu, T., Kasumi, H., Komori, S., and Koyama, K. (2008) CD52 is synthesized in cumulus cells and secreted into the cumulus matrix during ovulation. *Am. J. Reprod. Immunol.* **60**, 187–191
38. Yeung, C. H., Sonnenberg-Riethmacher, E., and Cooper, T. G. (1999) Infertile spermatozoa of c-ros tyrosine kinase receptor knockout mice show flagellar angulation and maturational defects in cell volume regulatory mechanisms. *Biol. Reprod.* **61**, 1062–1069
39. Florman, H. M., Corron, M. E., Kim, T. D., and Babcock, D. F. (1992) Activation of voltage-dependent calcium channels of mammalian sperm is required for zona pellucida–induced acrosomal exocytosis. *Dev. Biol.* **152**, 304–314
40. De La Vega-Beltran, J. L., Sánchez-Cárdenas, C., Krapf, D., Hernandez-González, E. O., Wertheimer, E., Treviño, C. L., Visconti, P. E., and Darszon, A. (2012) Mouse sperm membrane potential hyperpolarization is necessary and sufficient to prepare sperm for the acrosome reaction. *J. Biol. Chem.* **287**, 44384–44393
41. Kopcow, H. D., Rosetti, F., Leung, Y., Allan, D. S. J., Kutok, J. L., and Strominger, J. L. (2008) T cell apoptosis at the maternal–fetal interface in early human pregnancy, involvement of galectin-1. *Proc. Natl. Acad. Sci. USA* **105**, 18472–18477
42. Lee, M. Y., Lee, S. H., Park, J. H., and Han, H. J. (2009) Interaction of galectin-1 with caveolae induces mouse embryonic stem cell proliferation through the Src, ERas, Akt and mTOR signaling pathways. *Cell. Mol. Life Sci.* **66**, 1467–1478
43. Karmakar, S., Cummings, R. D., and McEver, R. P. (2005) Contributions of Ca^{2+} to galectin-1-induced exposure of phosphatidylserine on activated neutrophils. *J. Biol. Chem.* **280**, 28623–28631
44. Walzel, H., Brock, J., Pöhland, R., Vanselow, J., Tomek, W., Schneider, F., and Tiemann, U. (2004) Effects of galectin-1 on regulation of progesterone production in granulosa cells from pig ovaries *in vitro*. *Glycobiology* **14**, 871–881
45. Cohen, R., Buttke, D. E., Asano, A., Mukai, C., Nelson, J. L., Ren, D., Miller, R. J., Cohen-Kutner, M., Atlas, D., and Travis, A. J. (2014) Lipid modulation of calcium flux through CaV2.3 regulates acrosome exocytosis and fertilization. *Dev. Cell* **28**, 310–321
46. Wang, J., Lu, Z.-H., Gabius, H.-J., Rohowsky-Kochan, C., Ledeen, R. W., and Wu, G. (2009) Cross-linking of GM1 ganglioside by galectin-1 mediates regulatory T cell activity involving TRPC5 channel activation: possible role in suppressing experimental autoimmune encephalomyelitis. *J. Immunol.* **182**, 4036–4045
47. Poirier, F., and Robertson, E. J. (1993) Normal development of mice carrying a null mutation in the gene encoding the L14 S-type lectin. *Development* **119**, 1229–1236
48. Okabe, M., and Cummins, J. M. (2007) Mechanisms of sperm-egg interactions emerging from gene-manipulated animals. *Cell. Mol. Life Sci.* **64**, 1945–1958
49. Yeung, C.-H., Callies, C., Rojek, A., Nielsen, S., and Cooper, T. G. (2009) Aquaporin isoforms involved in physiological volume regulation of murine spermatozoa. *Biol. Reprod.* **80**, 350–357
50. Chen, Q., Peng, H., Lei, L., Zhang, Y., Kuang, H., Cao, Y., Shi, Q.-X., Ma, T., and Duan, E. (2011) Aquaporin3 is a sperm water channel essential for postcopulatory sperm osmoadaptation and migration. *Cell Res.* **21**, 922–933
51. Figueiras-Fierro, D., Acevedo, J. J., Martínez-López, P., Escoffier, J., Sepúlveda, F. V., Balderas, E., Orta, G., Visconti, P. E., and Darszon, A. (2013) Electrophysiological evidence for the presence of cystic fibrosis transmembrane conductance regulator (CFTR) in mouse sperm. *J. Cell. Physiol.* **228**, 590–601
52. Yeung, C.-H., Anapolski, M., Sipilä, P., Wagenfeld, A., Poutanen, M., Huhtaniemi, I., Nieschlag, E., and Cooper, T. G. (2002) Sperm volume regulation: maturational changes in fertile and infertile transgenic mice and association with kinematics and tail angulation. *Biol. Reprod.* **67**, 269–275
53. Jin, M., Fujiwara, E., Kakiuchi, Y., Okabe, M., Satouh, Y., Baba, S. A., Chiba, K., and Hirohashi, N. (2011) Most fertilizing mouse spermatozoa begin their acrosome reaction before contact with the zona pellucida during *in vitro* fertilization. *Proc. Natl. Acad. Sci. USA* **108**, 4892–4896
54. Cha, S.-K., Ortega, B., Kurosu, H., Rosenblatt, K. P., Kuro-O, M., and Huang, C.-L. (2008) Removal of sialic acid involving Klotho causes cell-surface retention of TRPV5 channel via binding to galectin-1. *Proc. Natl. Acad. Sci. USA* **105**, 9805–9810
55. Copits, B. A., Vernon, C. G., Sakai, R., and Swanson, G. T. (2014) Modulation of ionotropic glutamate receptor function by vertebrate galectins. *J. Physiol.* **592**, 2079–2096
56. Santi, C. M., Martínez-López, P., de la Vega-Beltrán, J. L., Butler, A., Alisio, A., Darszon, A., and Salkoff, L. (2010) The SLO3 sperm-specific potassium channel plays a vital role in male fertility. *FEBS Lett.* **584**, 1041–1046
57. Yang, C., Zeng, X.-H., Zhou, Y., Xia, X.-M., and Lingle, C. J. (2011) LRRC52 (leucine-rich-repeat-containing protein 52), a testis-specific auxiliary subunit of the alkalization-activated Slo3 channel. *Proc. Natl. Acad. Sci. USA* **108**, 19419–19424
58. Zeng, X.-H., Yang, C., Xia, X.-M., Liu, M., and Lingle, C. J. (2015) SLO3 auxiliary subunit LRRC52 controls gating of sperm KSPER currents and is critical for normal fertility. *Proc. Natl. Acad. Sci. USA* **112**, 2599–2604

Received for publication January 26, 2015.
Accepted for publication June 8, 2015.